Dynamic Characteristic Parameters Analysis of Radial-thrust Film Bearing

Hao Zhang[1], Shuo Han[2], Jiwu Li[2] and Qingkai Han[1,2*]

1. Collaborative Innovation Center of Major Machine Manufacturing in Liaoning, Dalian University of Technology, Dalian,116024, China
2. School of Mechanical Engineering, Dalian University of Technology, Dalian, 116024, China

Abstract: Radial-thrust film bearing can carry radial and axial loads simultaneously, and are widely used in special structure with limited space. In this paper, a certain type of radial-thrust film bearing is studied based on the fluid Reynolds equation and the force balance assumption. Then the dynamic parameters of bearing film and thrust surface under the different load and extrusion speeds are analysis. Finally, the approximate stiffness and the change rules of damping coefficient under different loads and rotational speeds are obtained. The results can provide theoretical support for the dynamic optimization design of the rotor system with radial-thrust film bearing.

Keywords: Radial-thrust film bearing; Nonlinear oil film force; Dynamic characteristic parameter

1 Introduction

Oil film bearing is the core component of the large-scale mechanical equipment such as compressor and so on, which has typical nonlinear characteristics. The dynamic characteristics of oil film bearing have a very obvious influence on the working performance of the rotor system and the whole equipment. The radial-thrust film bearing, as a kind of composite bearing, can carry both radial and axial loads at the same time. It is widely used in the special and the space limited situation where the axial force and radial force exist at the same time. Dynamic analysis of this kind of bearing to master the nonlinear relationship between the oil film force and the load, speed is significant to the dynamics design of the rotor system.

At present, two methods are used in the numerical calculation of the bearing rotor system. One is to directly calculate the oil film force and take it into the equation to iterate. The other one is to approximate the oil film force to the dynamic characteristic parameters of the oil film, that is, the oil film stiffness and damping are used to express the oil film dynamic characteristics. In the first method, the dynamic oil film force of the bearing is more time-consuming by using the finite element method or the

* Corresponding author: (hanqingkai@dlut.edu.cn)

variation method. Therefore, the Reynolds equation is often solved by using reasonable boundary conditions in analysing and solving practical problems. The infinite length hypothesis of the bearing oil film force model proposed by Sommerfeld and the short bearing hypothesis proposed by Capone are most representative. For example, Chang-Jian[1] used long bearing hypothesis to calculated the nonlinear dynamic characteristics of the disc rotor system supported by a circular tile bearing, and Amamou[2] analysed the dynamic stability of the circular tile bearing with the hypothesis of long bearing. Lin[3] used the short bearing hypothesis to analyzed the lubrication characteristics of bearings under Non-Newtonian ferrofluid. Soni[4] used the short bearing hypothesis to analyzed the nonlinear dynamic characteristics of circular bearing under thin film lubrication. Due to the complex calculation process, the first calculation method is not very common in engineering application. But in the second method, it can be easily calculated after obtaining the dynamic characteristic parameters of the oil film force and widely used in the critical speed calculating of the rotor system. For example, Glienicke[5] and Allaire[6] systematically discussed the calculation method of the dynamic coefficient of oil film bearing, and give the non-dimensional stiffness and damping coefficient of different types of radial bearings. Barrett[7] used the eight coefficients dynamic characteristic model to solve the critical speed of the five watts tilting bearing rotor system under steady load. Mittwollen[8] studied the calculation method of the oil film thrust bearing dynamic characteristic parameters at high speed, and obtained the influence law of the oil film thrust bearing dynamic characteristics on the radial vibration of the high-speed rotating rotor system. Srikanth[9,10] ignored the freedom degree of the tile of tilting tile thrust bearing, and solved the nonlinear stiffness and damping parameters of tilting tile thrust bearings with different sizes.

In the current engineering design process, the dynamic characteristic parameters of the oil film bearing under the working speed and the working load are generally used to analyze the dynamic characteristics, and the dynamic characteristics obtained of the system are often linear. However, because of the coupling effect between the bearing rotors, some nonlinear behavior of the bearing may be excited in a certain excitation range. This simplified method may ignore some important dynamic characteristics of the bearing and bring security risks to the designed products.

In this paper, the nonlinear characteristics of the bearing based on the parameters of a radial-thrust bearing are studied. With the hypothesis of the static balance, the dynamic calculation method of the dynamic parameters of the bearing are proposed, and the characteristics of the bearing under different speeds and loads are obtained, which would provide support for the dynamic design of the rotor system.

2 Nonlinear force of radial-thrust film bearing

2.1 Dynamic modeling of radial-thrust film bearing

A radial-thrust film bearing, as shown in Fig. 1, is a bearing with a radial bearing and an axial thrust bearing, which is constituted with a supporting surface (cylindrical

 ISSN 2572-4975 (Print), 2572-4991 (Online)

pad oil film bearing) and a thrust surface (slanted-plane sector fixed pad thrust bearing).

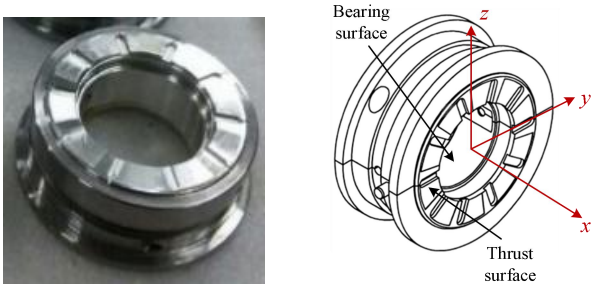

Fig.1. A radial-thrust film bearing

The bearing surface dynamic model is shown in Fig. 2. Where, the journal is rotated with a rotational speed Ω under the effect of a stable load F; O and O_b are the center of the journal and the bearing respectively; r is the radius of the journal; R_b is the radius of the inner bearing; φ is the deflection angle of the journal, and e is eccentricity; $h(\theta)$ is the clearance function that represents the oil film thickness; θ is the circumferential coordinate of the bearing; $h_{\max}$ is the largest radial clearance of the bearing; $h_{\min}$ is the smallest radial clearance of bearing.

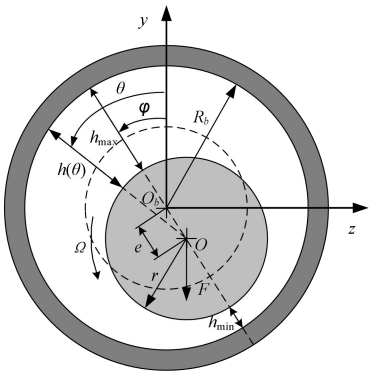

Fig.2. Dynamic model of the bearing surface

The thickness θ of the oil film at the journal can be expressed as

$$h(\theta) = C + e\cos(\theta - \varphi) = C - y\cos\theta + z\sin\theta \quad (1)$$

where, y and z are the horizontal and vertical displacement of the journal respectively, and C is the radius clearance of the bearing, and expressed as

$$C = R_b - r \quad (2)$$

The boundary condition of oil film with semi Sommerfeld boundary condition can be expressed as

$$\begin{cases} p(\theta_1, x) = p(\theta_2, x) = 0 \\ p(\theta, -\frac{L}{2}) = p(\theta, \frac{L}{2}) = 0 \end{cases} \tag{3}$$

Among them, θ_1 and θ_2 are the starting and ending boundary angles of the circumferential oil film, and L is the width of the bearing.

The Reynolds equation used for oil film analysis of bearings is obtained through coordinate transformation.

$$\frac{1}{R_b^2}\frac{\partial}{\partial\theta}\left(\frac{h^3}{12\eta}\frac{\partial p}{\partial\theta}\right)+\frac{\partial}{\partial x}\left(\frac{h^3}{12\eta}\frac{\partial p}{\partial x}\right)=\frac{1}{2}\Omega\frac{\partial h}{\partial\theta}+\frac{\partial h}{\partial t} \tag{4}$$

where, η is the dynamic viscosity(Ns/m^2) of lubricating oil, p is oil film pressure(N/m^2) and the x is the coordinate position along the bearing width.

Through the nondimensionalization, Eq.(4) can be transformed into

$$\frac{\partial}{\partial\theta}\left(\overline{h}^3\frac{\partial\overline{p}}{\partial\theta}\right)+\lambda^2\frac{\partial}{\partial\overline{x}}\left(\overline{h}^3\frac{\partial\overline{p}}{\partial\overline{x}}\right)=-\overline{e}\sin(\theta-\varphi)+2\dot{\overline{e}}\cos(\theta-\varphi_{\mathrm{de}})=f(\theta) \tag{5}$$

where, $\overline{p}=p/[6\eta\Omega(R_b/\mathrm{C})^2]$, $\overline{x}=x/(L/2)$, $\lambda=2R_b/L$, $\overline{e}=e/C$, $\dot{\overline{e}}=\dot{e}/(C\Omega)$, $\overline{h}=h/C=1+\overline{e}\cos(\theta-\varphi)$, $\tau=\Omega t$.

The thrust surface is composed of many sector surfaces, and the sector surface can be regarded as a thrust pad. The dynamic model of the single fixed thrust pad is shown in Fig. 3.

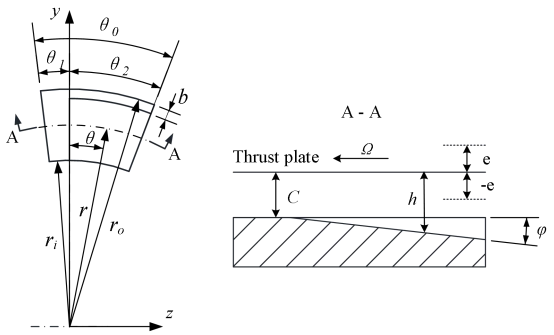

Fig.3. Dynamic model of thrust surface

In Fig. 3, θ_0 is the sector width angle; θ_1 is the wedge width angle, the sealing width is b; the inner radius of pad is r_i; the outer radius of the pad is r_o; θ and r are the circumferential and radial coordinates of the pads respectively; $h(\theta)$ is the thickness of the oil film in the circumferential coordinates θ; C is the bearing clearance; e is relative displacement between thrust plate and bearing end face.

The oil film thickness at any point above the end face can be expressed as

$$h(\theta,r)=\begin{cases} C+e-r\sin\theta\sin\varphi & \theta<0 \text{ and } r<r_o-b \\ C+e & \text{other} \end{cases} \tag{6}$$

ISSN 2572-4975 (Print), 2572-4991 (Online)

The boundary condition of the oil film of the Reynolds equation can be expressed as

$$\begin{cases} p(r_i,\theta) = p(r_o,\theta) = 0 \\ p(r,\theta_1) = p(r,\theta_2) = 0 \end{cases} \tag{7}$$

where, θ_1 and θ_2 are the circumferential starting and ending boundary angles of oil film .

The Reynolds equation for oil film analysis on each sector surface is

$$\frac{1}{r^2}\frac{\partial}{\partial\theta}\left(\frac{h^3}{12\eta}\frac{\partial p}{\partial\theta}\right)+\frac{\partial}{\partial r}\left(\frac{h^3}{12\eta}\frac{\partial p}{\partial r}\right)=\frac{1}{2}\Omega\frac{\partial h}{\partial\theta}+\frac{\partial h}{\partial t} \tag{8}$$

Through the nondimensionalization, Eq.(8) can be transformed into

$$\kappa^2\frac{\partial}{\partial\theta}\left(\overline{h}^3\frac{\partial\overline{p}}{\partial\theta}\right)+\frac{\partial}{\partial\overline{r}}\left(\overline{h}^3\frac{\partial\overline{p}}{\partial\overline{r}}\right)=\frac{\partial\overline{h}}{\partial\theta}+2\frac{\partial\overline{h}}{\partial\tau} \tag{9}$$

where, $\overline{p}=p/[6\eta\Omega(r_i/\mathrm{C})^2]$, $\overline{r}=r/r_i$, $\overline{b}=b/r_i$, $\overline{h}=h/C$, $\overline{e}=e/C$, $\dot{\overline{e}}=\dot{e}/(C\Omega)$, $\tau=\Omega t$, $\kappa=1/\overline{r}$.

2.2 The relationship between the bearing force and the journal offset

The structural parameters and working parameters of the bearing, which shown in Fig. 1, are shown in Table 1.

Table 1. Main parameters of bearing

Inner diameter of support surface D_b mm	50
Radius clearance of bearing surface C mm	0.025
The bearing surface width L mm	25
the outer radius of the pad r_o mm	40
the inner radius of pad r_i mm	28
The number of thrust surface pads n	10
Thrust surface mounting clearance C mm	0.015
Thrust surface pad angle θ_0 deg	28
Area angle of wedge surface of thrust surface θ_1 deg	21
Wedge surface angle of thrust surface φ deg	25
Width of sealing surface of thrust surface b mm	3
Working speed r/min	2600
Maximum speed r/min	3000
Lubricating oil viscosity η Pa.s or kg/(ms)(40℃)	0.028

The negative pressure along the y axis is applied. Taking bearing in Table 1 as an example, the relationship between the journal displacement, the deviation angle and the load was obtained by differential method, as shown in Fig. 4. When the load was 1kN and 10kN, the distribution of the circumferential pressure of the bearing is shown in Fig. 5.

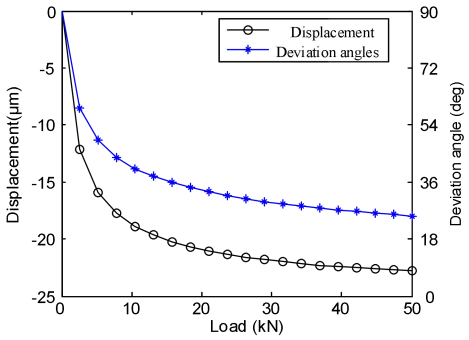

Fig.4. Displacements and deviation angles of the journal bearing under different loads

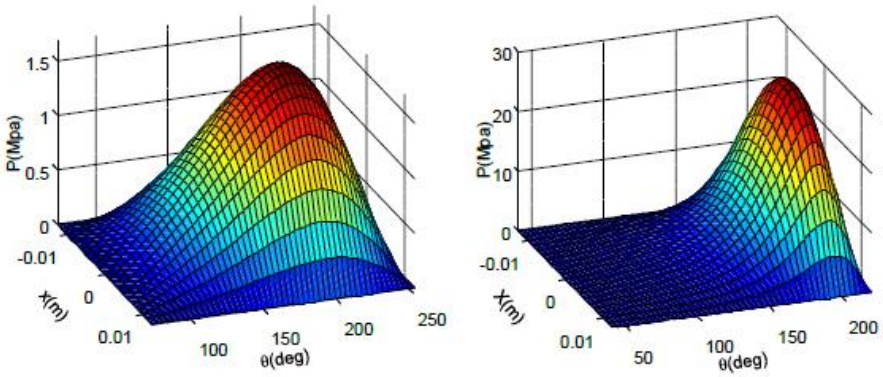

(a) Pressure distribution when load is 1kN (b) Pressure distribution when load is 10kN

Fig. 5. Pressure distribution of the journal bearing under different loads

In Fig. 4, it can be seen that the displacement of the journal increases with the increase of the load. While the deviation angle decreases with the increase of the load gradually from 90°, but all of them changed slowly due to the increase of the stiffness of the oil film. When load is below 10kN, the variation of journal displacement and deflection is sensitive to load change. In Fig. 5, it can be seen that after the pressure increases 10 times, the maximum pressure of the fluid is increased by 17 times. The increase of the load will make the circumferential pressure distribution of the bearing lubricating oil more uneven, and the local pressure increases sharply.

According to the axial pressure applied to the bearing, the relationship between axial displacement and axial load is obtained by differential method, as shown in Fig.

ISSN 2572-4975 (Print), 2572-4991 (Online)

6. The pressure distribution on the thrust surface of the bearing under the load is 1kN and 5kN is shown in Fig. 7.

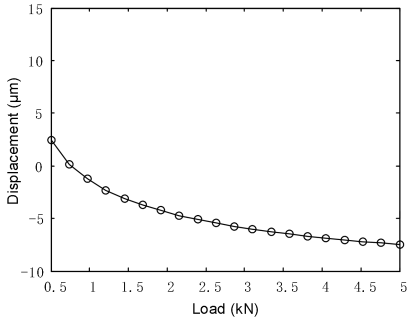

Fig.6. Displacements of thrust bearing vs loads under rated speed

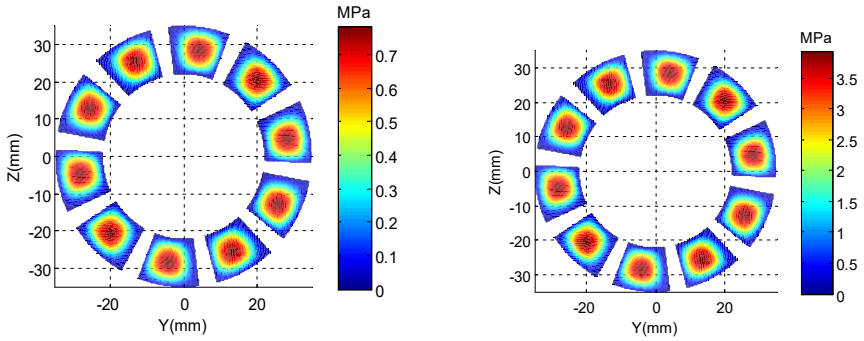

(a) The load is 1kN (b) The load is 5kN

Fig.7. Pressure distribution of the thrust bearing I under different loads

Fig. 6 shows that the oil film thickness between the thrust face and the thrust face decreases as the load increases, but the decrease gradually slows down. The oil film thickness is significantly related to the rotational speed. Under the same load condition, the higher the rotating speed of the journal, the greater the thickness of the oil film. In Fig. 7, it can be seen that the maximum pressure of the fluid increases about 5 times after the pressure increases 5 times, and the pressure load has little effect on the distribution of the lubricating oil pressure in the thrust surface of the bearing.

2.3 Effect of oil film bearing extrusion speed on oil film force

In the unsteady operation of the radial oil film bearing, the oil film force will also produce unstable changes due to the oscillation of the journal. When the bearing at the rated speed, the initial vertical load is 1.6kN. At this time, the displacement is 4μm and the displacement declination is 77.5°. The influence of the journal oscillation on

the oil film bearing force of the oil film bearing is shown in Fig 8(a). If the initial vertical load of the bearing 3 is 4.1kN, the displacement is 8μm and the displacement declination is 25.2°. The influence of the journal oscillation on the oil film bearing force of the oil film bearing is shown in Fig. 8(b).

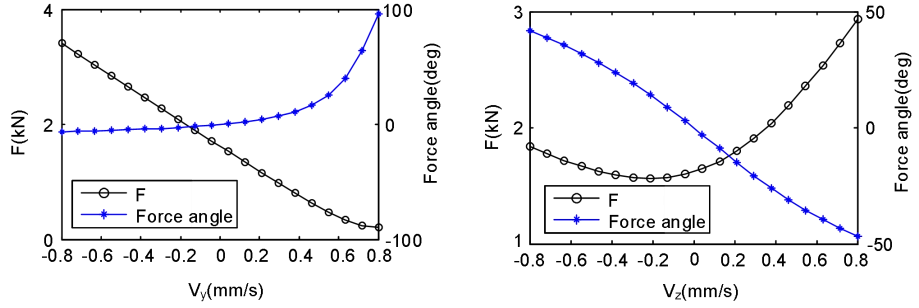

(a) The load is 1.6kN

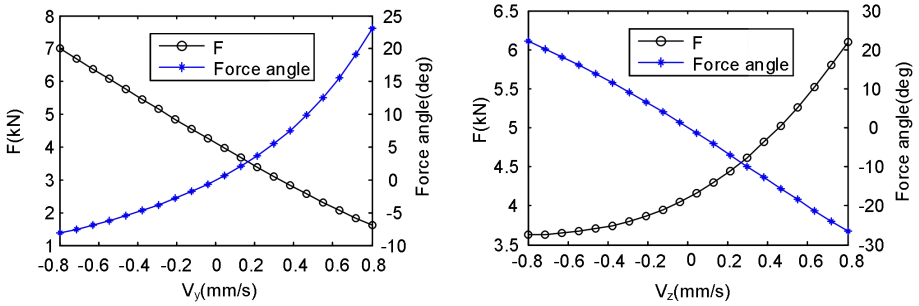

(b) The load is 4.1kN

Fig. 8. Relationship between oil film force, offset angle and journal extrusion speed of bearing surface

It can be seen from Fig. 8(a) that when the journal vibrates in the y direction, the oil film force decreases with the increase of the vibration speed, and is approximately linearly distributed in the range of -0.8 mm/s to 0.8 mm/s, while the oil film force deviation angle increases as the vibration speed increases. When the journal vibrates in the z direction, the oil film force first decreases and then increases with the increase of the vibration speed, while the oil film force deviation angle decreases with the increase of the journal vibration speed, and is approximately linear distributed. It can be seen from Fig. 8(b), when the journal vibrates in the y direction, the trend of the oil film force and its deviation angle is consistent with the trend of Fig. 8(a), but the oil film force is more sensitive to the extrusion speed, and the range of the variation is also Bigger. When the journal vibrates in the z direction, the oil film force deviation angle is the same as that of Fig. 8(a), which is approximately linear. When the z-direction vibration velocity in the range of -0.8 mm/s to 0.8 mm/s, the oil force increases with the increase of the journal speed. Therefore, the vibration of the journal has a significant effect on the change of the oil film force. A small change in the extrusion speed tends to cause a multiple change in the journal force, and this effect is more obvious as the rotational speed increases.

ISSN 2572-4975 (Print), 2572-4991 (Online)

The effect of the axial vibration of the journal on the oil film force is analyzed for the bearing thrust surface under unsteady operation. Under the rated speed, the distance between the end face of the thrust plate and the thrust surface is 12μm. The influence of the journal oscillation on the oil film force of the oil film bearing is shown in Fig. 9(a). The initial pressure of each thrust surface is increased, and the distance between the end face of the thrust plate and the thrust surface is reduced to 9μm. The influence of the obtained journal oscillation on the oil film force of the oil film bearing is shown in Fig. 9(b).

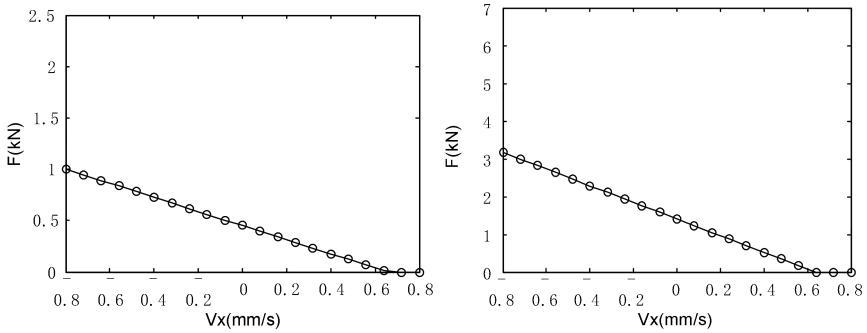

(a) When the minimum oil film thickness is 12μm

(b) When the minimum oil film thickness is 9μm

Fig. 9. Relationship between oil film force on thrust surface and extrusion speed of thrust plate

It can be seen from Fig. 9(a) that when the thrust disk vibrates in the axial direction, the oil film force decreases with the increase of the vibration speed, and is approximately linearly distributed. When the oil film pressure is negative, the oil film is broken and the bearing is ineffective. It can be seen from Fig. 9(b) that the same failure phenomenon occurs when the axial velocity coincides with Fig. 9(a). This is because when the axial velocity is greater than the derivative of the oil film thickness versus time dh/dt , the oil film cannot be formed. Therefore, when the speed is constant, regardless of the static pressure, it will fail at a fixed extrusion speed.

3 The parameter analysis of bearing dynamic characteristics

3.1 Calculation method of oil film dynamic characteristic parameters

For the radial-thrust film bearing shown in Fig.1, if the coupling effect between the bearing surface and the thrust surface is neglected, based on the static balance assumption, Taylor expansion is performed at the static equilibrium position and the first two steps are taken. The force approximation is represented by the stiffness and damping characteristic parameters, as shown in Eq. (10).

$$\begin{Bmatrix} F_x \\ F_y \\ F_z \end{Bmatrix} = \begin{Bmatrix} F_{x0} \\ F_{y0} \\ F_{z0} \end{Bmatrix} + \begin{bmatrix} k_{xx} & & \\ & k_{yy} & k_{yz} \\ & k_{zy} & k_{zz} \end{bmatrix} \begin{Bmatrix} x \\ y \\ z \end{Bmatrix} + \begin{bmatrix} c_{xx} & & \\ & c_{yy} & c_{yz} \\ & c_{zy} & c_{zz} \end{bmatrix} \begin{Bmatrix} \dot{x} \\ \dot{y} \\ \dot{z} \end{Bmatrix} = \boldsymbol{F}_0 + \boldsymbol{KX} + \boldsymbol{C\dot{X}} \quad (10)$$

where, F_0 is the static load force; K is the stiffness characteristic parameter of the bearing; C is the damping characteristic parameter of the bearing. The oil film dynamic parameters are analyzed from the bearing surface and the thrust surface, respectively.

For the bearing surface, when the journal is running smoothly, it will be subjected to a stable oil film force and in a static equilibrium position (e_0, φ_0). At this time, the oil film thickness is $h_0(\theta)$ and the oil film pressure is p_0, and there is

$$\begin{Bmatrix} F_y \\ F_z \end{Bmatrix} = \begin{Bmatrix} F_{y0} \\ F_{z0} \end{Bmatrix} + \begin{bmatrix} k_{yy} & k_{yz} \\ k_{zy} & k_{zz} \end{bmatrix} \begin{Bmatrix} y \\ z \end{Bmatrix} + \begin{bmatrix} c_{yy} & c_{yz} \\ c_{zy} & c_{zz} \end{bmatrix} \begin{Bmatrix} \dot{y} \\ \dot{z} \end{Bmatrix} \tag{11}$$

Set the oil film thickness change caused by the small displacement Δy, Δz to

$$h = h_0 - \Delta y \cos\theta + \Delta z \sin\theta \tag{12}$$

The corresponding oil film pressure can be developed according to the Taylor formula.

$$p \approx p_0 + \frac{\partial p}{\partial y}\Delta y + \frac{\partial p}{\partial z}\Delta z + \frac{\partial p}{\partial \dot{y}}\Delta \dot{y} + \frac{\partial p}{\partial \dot{z}}\Delta \dot{z} \tag{13}$$

Introduced by Eq. (5)

$$\frac{\partial}{\partial\theta}\left(\bar{h}_0^3 \frac{\partial \bar{p}'}{\partial\theta}\right) + \lambda^2 \frac{\partial}{\partial \bar{x}}\left(\bar{h}_0^3 \frac{\partial \bar{p}'}{\partial \bar{x}}\right)$$

$$= \begin{cases} \left(\sin\theta + 3\dfrac{\cos\theta}{\bar{h}_0}\dfrac{\partial \bar{h}_0}{\partial\theta}\right) - 3\bar{h}_0^2\left(\sin\theta + \dfrac{\cos\theta}{\bar{h}_0}\dfrac{\partial \bar{h}_0}{\partial\theta}\right)\dfrac{\partial \bar{p}_0}{\partial\theta} & \text{when } \bar{p}_i' = \dfrac{\partial \bar{p}}{\partial \bar{y}} \\ \left(\cos\theta - 3\dfrac{\sin\theta}{\bar{h}_0}\dfrac{\partial \bar{h}_0}{\partial\theta}\right) - 3\bar{h}_0^2\left(\cos\theta - \dfrac{\sin\theta}{\bar{h}_0}\dfrac{\partial \bar{h}_0}{\partial\theta}\right)\dfrac{\partial \bar{p}_0}{\partial\theta} & \text{when } \bar{p}_i' = \dfrac{\partial \bar{p}}{\partial z} \\ -2\cos\theta & \text{when } \bar{p}_i' = \dfrac{\partial \bar{p}}{\partial \dot{\bar{y}}} \\ 2\sin\theta & \text{when } \bar{p}_i' = \dfrac{\partial \bar{p}}{\partial \dot{\bar{z}}} \end{cases} \tag{14}$$

The above equations can be integrated in the complete oil film region by the difference equation form to obtain the coefficients in Eq.(11), and then integrated again to obtain the increments of the oil film force, that is, the stiffness and damping dynamic characteristic coefficients are

$$\begin{bmatrix} k_{yy} & k_{yz} \\ k_{zy} & k_{zz} \end{bmatrix} = \int_{-\frac{L}{2}}^{\frac{L}{2}} \int_{\theta_1}^{\theta_2} \begin{bmatrix} \dfrac{\partial p}{\partial y}\cos\theta & -\dfrac{\partial p}{\partial y}\sin\theta \\ \dfrac{\partial p}{\partial z}\cos\theta & -\dfrac{\partial p}{\partial z}\sin\theta \end{bmatrix} R_b d\theta dx$$

$$\begin{bmatrix} c_{yy} & c_{yz} \\ c_{zy} & c_{zz} \end{bmatrix} = \int_{-\frac{L}{2}}^{\frac{L}{2}} \int_{\theta_1}^{\theta_2} \begin{bmatrix} \dfrac{\partial p}{\partial \dot{y}}\cos\theta & -\dfrac{\partial p}{\partial \dot{y}}\sin\theta \\ \dfrac{\partial p}{\partial \dot{z}}\cos\theta & -\dfrac{\partial p}{\partial \dot{z}}\sin\theta \end{bmatrix} R_b d\theta dx \tag{15}$$

ISSN 2572-4975 (Print), 2572-4991 (Online)

For the thrust surface, when the thrust plate runs smoothly, it will receive a stable oil film force and be in a static equilibrium position. At this time, the oil film thickness is h_0, the oil film pressure is p_0, there is

$$F_x \approx F_{x0} + \left.\frac{dF_x}{dx}\right|_0 \Delta x + \left.\frac{dF_x}{d\dot{x}}\right|_0 \Delta\dot{x} = F_{x0} + k_{xx}\Delta x + c_{xx}\Delta\dot{x} \tag{16}$$

In the formula, k_{xx} and c_{xx} are the stiffness and damping coefficient of the thrust surface oil film.

Let the oil film thickness change caused by the small displacement Δx be

$$h = h_0 - \Delta x \tag{17}$$

The corresponding oil film pressure can be developed according to the Taylor formula.

$$p \approx p_0 + \frac{dp}{dx}\Delta x + \frac{dp}{d\dot{x}}\Delta\dot{x} \tag{18}$$

Introduced by Eq. (9)

$$\kappa^2 \frac{\partial}{\partial\theta}\left(\bar{h}_0^3 \frac{\partial\bar{p}'}{\partial\theta}\right) + \frac{\partial}{\partial\bar{r}}\left(\bar{h}_0^3 \frac{\partial\bar{p}'}{\partial\bar{r}}\right) = \begin{cases} -\dfrac{3}{\bar{h}_0}\dfrac{\partial\bar{h}_0}{\partial\theta} + 3\bar{h}_0\left[\kappa^2 \dfrac{\partial\bar{p}_0}{\partial\theta}\dfrac{\partial\bar{h}_0}{\partial\theta} + \dfrac{\partial\bar{p}_0}{\partial\bar{r}}\dfrac{\partial\bar{h}_0}{\partial\bar{r}}\right] & \text{when } \bar{p}_i' = \dfrac{d\bar{p}}{d\bar{x}} \\ 2 & \text{when } \bar{p}_i' = \dfrac{d\bar{p}}{d\dot{\bar{x}}} \end{cases} \tag{19}$$

The above equations can be integrated in the complete oil film region by the difference equation form to obtain the coefficients in Eq.(16), and then integrated again to obtain the increments of the oil film force, that is, the dynamic characteristic coefficient is

$$\begin{aligned} k_{xx} &= -\int_{r_i}^{r_o}\int_{\theta_1}^{\theta_2} \frac{\partial p}{\partial x} r\,d\theta dr \\ c_{xx} &= -\int_{r_i}^{r_o}\int_{\theta_1}^{\theta_2} \frac{\partial p}{\partial \dot{x}} r\,d\theta dr \end{aligned} \tag{20}$$

3.2 Analysis of oil film dynamic characteristics of bearings

According to the Eqs. (15) and (20), the bearing shown in Table 1 was analyzed, and the relationship between the stiffness characteristic and the damping characteristic parameter and the load and the journal rotation speed is obtained as shown in Figs. 10 and 11.

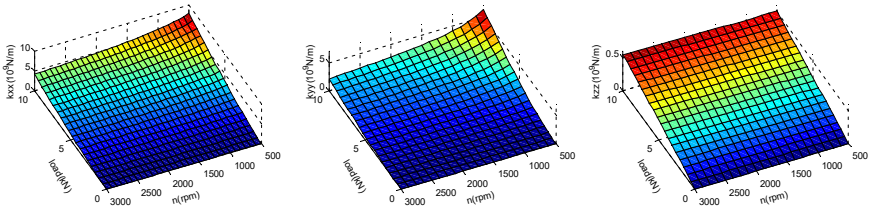

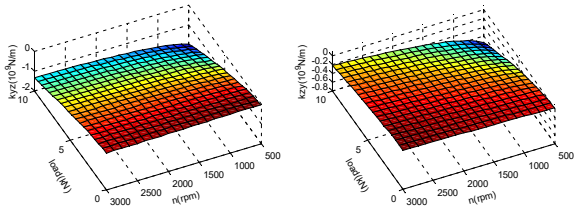

Fig.10. Bearing stiffness coefficient

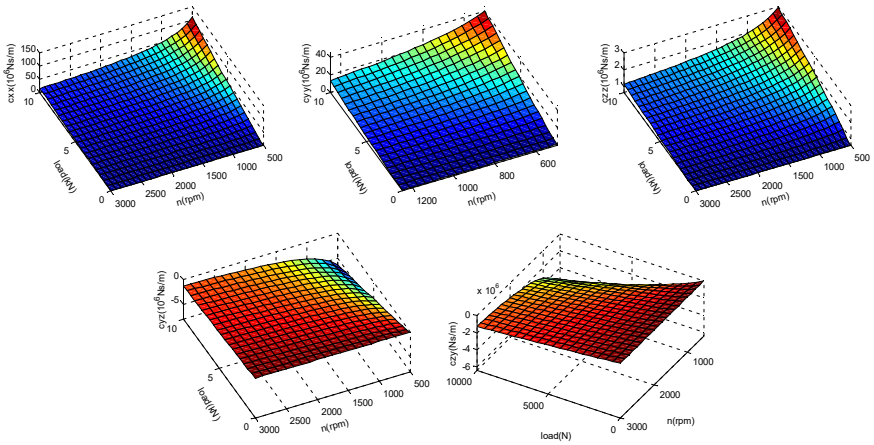

Fig.11. Bearing damping coefficient

It can be seen that when the rotational speed is constant, k_{yy} and k_{zz} increases with the increase of the bearing load, k_{yz} and k_{zy} decreases with the increase of the bearing load; When the load is constant, k_{yy} and k_{zz} decreases with the increase of the journal speed, and k_{yz} and k_{zy} increases with the increase of the journal speed. Compared with k_{zz} , Because k_{yy} is consistent with the load direction, the change is more affected by the load and the speed. Under low speed and heavy load, the stiffness k_{yy} in the load direction is much larger than the vertical stiffness k_{zz} .The value of k_{yz} is constant less than 0, and the sign symbol of k_{zy} depends on the speed and load. Under low speed and heavy load, the value of k_{zy} is negative, while at high speed and light load, the value of k_{zy} is positive. Also under the influence of load and speed, the rate of change of cross k_{yz} is less than k_{zy} . As can be seen in Fig. 11, the damping coefficients c_{yy} and c_{zz} increased as the bearing load increased, and decreased as the journal speed increased. The c_{yz} is equal to c_{zy} , and it's value decreases as the load increased and increased as the rotation speed increased, and it is always less than

 ISSN 2572-4975 (Print), 2572-4991 (Online)

0 when the load is applied. At the same time, the stiffness damping parameter of the thrust surface is consistent with the main stiffness coefficient and the main damping coefficient of the bearing, and both of them increased with the increased of the load and decreased with the increased of the rotational speed. Under the same load, the dynamic coefficient of the thrust surface is significantly larger than that of the cylindrical oil film bearing.

4 Conclusions

Based on the two-dimensional Reynolds equation, the mechanical properties of radial thrust combined oil film bearings are studied by finite difference method.

For the bearing support surface, the displacement of the journal increases with the increase of the radial load, and the offset angle decreases as the stiffness of the load increases. The increasing of the load would increase uneven distribution of pressure and causes a sharp increase in local pressure. In addition, the small vibration of the journal also has a significant effect on the change of the oil film force. A small extrusion speed tends to cause a multiplication of the journal force, and this effect is more obvious with the increase of the rotational speed.

For the thrust surface of the bearing, the thickness of the oil film decreases with the increase of the load and the decrease of the rotational speed. While the load has little effect on the pressure distribution of the thrust surface lubricant. When the thrust disk vibrates in the axial direction, the oil film force decreases with the increase of the vibration speed, and is approximately linear. When the axial velocity away from the thrust disk is greater than the derivative of the oil film thickness versus time dh/dt, the bearing fails.

The stiffness and damping coefficient of the bearing are monotonic functions with respect to the load and have obvious nonlinear characteristics.

Acknowledgements

This project is supported by National Natural Science Foundation of China (Grant No. 51705064).

References

1. C.J. C W, C.K. Chen, Bifurcation and Chaos Analysis of A Flexible Rotor Supported by Turbulent Long Journal Bearings, ***Chaos, Solitons & Fractals***, 34 (2007) 1160-1179.
2. A. Amamou, M. Chouchane, Nonlinear Stability Analysis of Long Hydrodynamic Journal Bearings using Numerical Continuation, ***Mechanism and Machine Theory***, 72(2014) 17-24.
3. J.R. Lin, P.J. Li, T.C. Hung, Lubrication Performances of Short Journal Bearings Operating with Non-Newtonian Ferrofluids, ***Z. Naturforsch***, 68(2013) 249-254.

4. S. Soni, D.P. Vakharia, Performance Analysis of Short Journal Bearing under Thin Film Lubrication, ***ISRN Mechanical Engineering***, (2014) Article ID 281021, 8 pages .
5. J. Glienicke, D.C. Han, Leonhard M. Practical Determination and Use of Bearing Dynamic Coefficients, ***Tribology international***, 13(6) (1980) 297-309.
6. P.E. Allaire, J.K. Parsell, L.E. Barrett, A Pad Perturbation Method for The Dynamic Coefficients of Tilting-Pad Journal Bearings, ***Wear***, 72(1) (1981) 29-44.
7. L.E. Barrett, P.E. Allaire, B.W. Wilson, The Eigenvalue Dependence of Reduced Tilting Pad Bearing Stiffness and Damping Coefficients. ***Tribology transactions***, 31(4) (1988) 411-419.
8. N. Mittwollen, T. Hegel, J. Glienicke, Effect of Hydrodynamic Thrust Bearings on Lateral Shaft Vibrations, ***Journal of tribology***, 113(4) (1991) 811-817.
9. D.V. Srikanth, K.K. Chaturvedi, A.C.K Reddy, Modelling of Large Tilting Pad Thrust Bearing Stiffness and Damping Coefficients, ***Tribology in industry***, 31(2009) 3-4.
10. D.V. Srikanth, Oil Film Angular Stiffness Determination in a Hydroelectric Tilting Pad Thrust Bearing, ***STLE/ASME 2010 International Joint Tribology Conference, American Society of Mechanical Engineers***, (2010)131-133.

 ISSN 2572-4975 (Print), 2572-4991 (Online)